Skin-friction estimation at high Reynolds numbers and Reynolds-number effects for transport aircraft

By A. Crook

1. Motivation and objectives

Accurate performance estimation is essential for any aircraft, either civil or military. Although both types of aircraft will operate at transonic cruise conditions for a portion of a typical flight, the civil transport aircraft is largely optimized for this condition above all others.

The purpose of this research brief is to conduct a brief review of skin-friction estimation over a range of Reynolds numbers, as this is one of the key parameters in performance estimation and Reynolds number scaling. If it is concluded that the available data are of insufficient quality, it is proposed to undertake an experiment to measure incompressible flat-plate skin friction directly over a large range of Reynolds numbers up to Reynolds numbers representative of flight conditions.

The flow around modern aircraft can be highly sensitive to Reynolds number. Elsenaar (1988a) provides a pragmatic criterion for defining sensitivity: "Reynolds number effects are large when they affect significantly the design (performance) of an aircraft as derived from sub-scale wind tunnel testing. Three drag counts variation in drag-creep will be significant for a transport type aircraft, but irrelevant for a maneuvering condition of a fighter aircraft." For a transport aircraft, the wing is the component most sensitive to Reynolds number change. Figure 1 shows the flow physics typically responsible for such sensitivity, which include boundary layer transition, shock / boundary-layer interaction and trailing-edge boundary-layer separation for transonic cruise conditions and the same features for a high-lift configuration in addition to confluent boundary layers, possible re-laminarization and leading-edge separation bubbles.

The nature of the interaction between a shock wave and an attached boundary layer depends largely upon whether the boundary layer is laminar or turbulent at the foot of the shock. For a laminar boundary layer, separation of the boundary layer will occur for a relatively weak shock and upstream of the freestream position of the shock. The majority of the pressure rise in this type of shock / boundary-layer interaction, generally described as a λ shock, occurs in the rear leg. The interaction of the rear leg with the separated boundary layer causes a fan of expansion waves that tend to turn the flow toward the wall, and hence re-attach the separated boundary layer. This is in contrast to the interaction between a turbulent boundary layer and a shock wave, in which the majority of the pressure rise occurs in the front leg of the shock wave. The expansion fan that causes reattachment of the laminar separated boundary layer is therefore not present, and the turbulent boundary layer has little tendency to re-attach.

Herein lies the problem of predicting the flight performance of an aircraft when the methods used to design the aircraft have historically relied upon wind tunnels operating below flight Reynolds number, together with other tools such as Computational Fluid Dynamics (CFD), empirical and semi-empirical methods and previous experience of similar design aircraft. Industrial wind tunnels such as the NASA 12ft and 11ft, Boeing Transonic

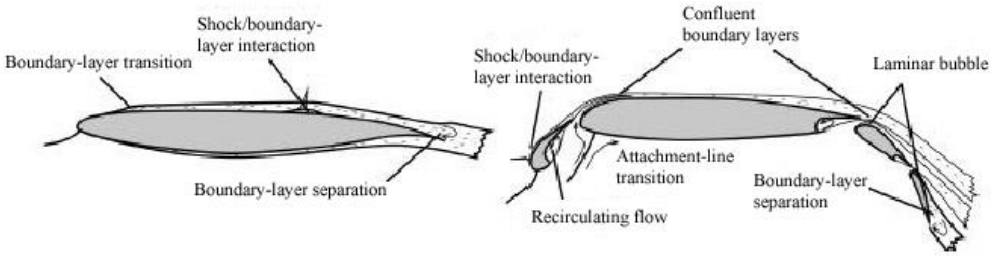

FIGURE 1. Flow features sensitive to Reynolds number for a cruise and high-lift configuration (Mack & McMasters (1992))

Wind Tunnel (BTWT) and the DERA (now QinetiQ) 5m can only achieve a maximum chord Reynolds number of between 3×10^6 and 16×10^6, compared with a typical value of 45×10^6 for cruise conditions. Therefore historically, results from wind tunnels have to be extrapolated to flight conditions in a process known as Reynolds-number scaling.

Comparison of wind tunnel and flight test results requires great caution as true Reynolds number effects, defined by Elsenaar (1988a) as the "change in flow development with Reynolds number for a particular configuration in free air," must be separated from scale and pseudo-Reynolds number effects that are a result of wind tunnel testing. Scale effects are characterised by Haines (1994) as those due to the model geometric fidelity and aeroelastic effects. The geometric fidelity of the model will not be as high as one would like because it is not possible to reproduce the many fine details of the aircraft at a small scale. This effect can be particularly important for military aircraft with external stores as discussed by Haines (1994), although it can be equally important for transport aircraft where the engines are not normally represented and the width of the slat and flap tracks may be larger than those scaled correctly, in order to withstand the high aerodynamic loads encountered in a high-lift configuration. Aeroelastic effects are also important because the model is rigid compared to the relatively flexible structure of the aircraft. The model wing is designed for 1g cruise conditions with the geometric twist matched to that of the wing at the same conditions in flight. Any deviation from this operating condition, such as a variation in the tunnel dynamic head (to vary Reynolds number) or C_L will mean that the twist of the model and aircraft wings will be different. Correction for aeroelastic effects must be made if the true Reynolds-number effects are to be shown.

Pseudo-Reynolds-number effects are related to the wind tunnel facility. Wind-tunnel models are generally supported rather than free flying and the flow around them is constrained by the tunnel walls, and therefore support and wall interference must be accounted for correctly. The freestream flow may also have a different turbulent length scale, turbulence intensity and spectrum to that occurring in the atmosphere. Other effects which can be wrongly interpreted as Reynolds number effects include the tunnel calibration, buoyancy effects, thermal equilibrium and humidity, as discussed by Haines (1994).

Haines & Elsenaar (1988) define two types of scale effect: indirect and direct, based upon the definition by Hall (1971) of scale effects being "the complex of interactions between the boundary layer development and the external inviscid flow." Direct and indirect Reynolds number effects are represented schematically in figure 2 and defined by Haines & Elsenaar (1988) as follows:

- Direct Reynolds-number effects occur as a consequence of a change in the boundary-

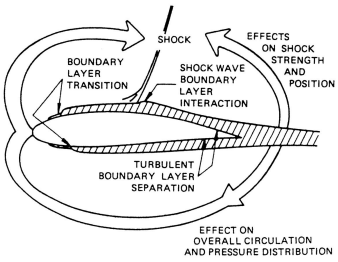

→ DIRECT REYNOLDS NUMBER EFFECT

⇒ INDIRECT REYNOLDS NUMBER EFFECT

DOMINANT RE-NUMBER EFFECT		
CHARACTERISTIC	DIRECT	INDIRECT
LIFT AND PITCHING MOMENT		X
VISCOUS DRAG	X	
WAVE DRAG		X
DRAG DIVERGENCE		X
BOUNDARY LAYER SEPARATION	X	
BUFFET BOUNDARY	X	X

FIGURE 2. Schematic representation of direct and indirect Reynolds number effects (Elsenaar (1988a))

layer development for a fixed (frozen) pressure distribution. Examples of "direct" effects range from the well-known variation of skin friction with Reynolds number for a given transition position to complex issues such as changes in the length of a shock-induced separation bubble for a given pressure rise through a shock

• Indirect Reynolds number effects are associated with changes in the pressure distribution arising from changes with Reynolds number in the boundary-layer and wake development. An example of an indirect effect is when changes in the boundary-layer displacement thickness with Reynolds number lead to changes in the development of supercritical flow, and hence in shock position and shock strength. Therefore, a change in wave drag with Reynolds number at a given C_L or incidence, can appear as an indirect Reynolds-number effect.

Haines (1987) provides a historical review of scale effects up to 1987, and gives examples of aircraft where direct effects dominated the wing flow, and indirect effects were probably small. The examples given are those of the VC-10 and X-1 aircraft, and correlation between wing pressure distributions in the wind tunnel and in flight are good. It is observed that the shock position in flight is slightly aft of that found in the tunnel test for these test conditions, when the flow is attached, with little or no trailing edge separation, and is turbulent. The reason for this behaviour in these two cases is the thinning of the boundary layer with increasing Reynolds number, with the displacement thickness being roughly proportional to $Re^{-\frac{1}{5}}$. The effective thickness of the wing therefore decreases and the effective camber increases with increasing Reynolds number. The shock wave will move downstream with reduced viscous effects until the limiting case of inviscid flow is reached. If however, C_L is kept constant for a given Mach number, and the Reynolds number varied, the increased aft loading must be compensated by a decrease in the load over the front of the aerofoil. This is generally accomplished by a decrease in the angle of incidence, which normally results in the forward movement of the shock wave. The final outcome of these opposing effects will depend upon their relative strength, as demonstrated by Elsenaar (1988b).

When the flow is attached or mostly attached, indirect Reynolds-number effects appear to be small. However, when the flow is separated large variations in the pressure

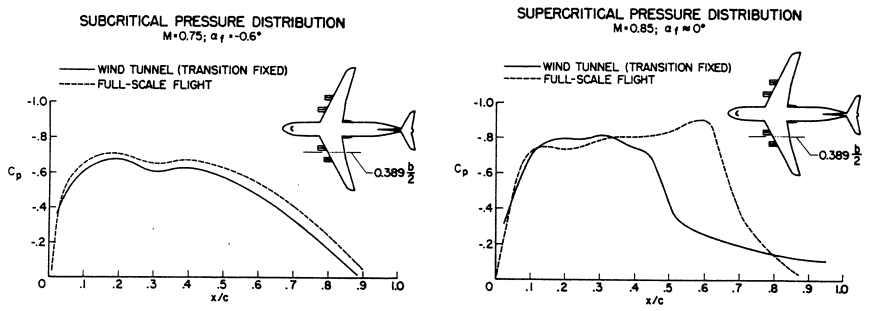

FIGURE 3. Comparison of C-141 wing pressure distributions between wind tunnel and flight for, (a) subcritical and (b) supercritical flow(Elsenaar (1988b))

distribution can result with varying Reynolds number *i.e.* indirect effects can be large as demonstrated in figure 3. Aside from the separation that can occur due to an adverse pressure gradient at the trailing edge, shock-boundary layer interaction is one of the primary causes of separation in transonic flight. Following the work of Pearcey *et al.* (1968) such flow separations are classed as either type A or B.

Elsenaar (1988b) describes the differences between type A and type B separation, and states that the final state is the same both, namely a boundary-layer separation from the shock to the trailing edge. However, the mechanism by which this final state is achieved, differs for the two. For a type A separation, the bubble that forms underneath the foot of the shock grows until it reaches the trailing-edge. The type B separation has three variants, with the common feature being a trailing edge separation that is present before the final state is reached. The final state is reached when the separation bubble and trailing-edge separation merge.

The type B separation is considered to be more sensitive to Reynolds number than type A. This is partly because the trailing-edge separation is dependent upon the boundary-layer parameters such as its thickness and displacement thickness. Furthermore, it was shown by Pearcey & Holder (1954) that the supersonic tongue that exists in a shock-boundary interaction is the dominant factor in the development of the separation bubble, and that the incoming boundary layer is less important. Moreover, the local shock Mach number that causes shock-induced separation is a weak function of the freestream Mach number. Relevant to wind tunnel-to-flight scaling is the possibility that at sufficiently high Reynolds numbers, the trailing edge separation will disappear and the type B flow that is observed in wind tunnels becomes a type A separation at flight conditions.

The behaviour of the trailing-edge separation and that of the separation bubble are highly coupled, with the trailing-edge separation amplified by the upstream effects of the shock-boundary layer interaction. The trailing-edge separation will modify the pressure distribution in a Reynolds-number-dependent manner, and this in turn will alter the shock strength and the conditions for separation at the foot of the shock. This will then affect the boundary layer at the trailing edge. The sensitivity to Reynolds number of this interaction process will be dependent upon the pressure distribution and hence the type of aerofoil (Elsenaar (1988b)). It is also argued that most pre-1960 aerofoils show a rapid increase in shock strength with increasing Mach number and angle of incidence. By implication viscous effects would be small, and the dominant effect would be lengthening of the shock-induced separation bubble. By contrast, modern supercritical aerofoils are designed to limit the variation in shock-wave strength and have higher aft loading and

hence greater pressure gradients over the rear of the aerofoil. Viscous effects will therefore be more important for these aerofoils and there performance more sensitive to Reynolds number.

As demonstrated by figure 3, estimation of aircraft performance and characteristics based upon data from wind-tunnel tests at low Reynolds number can lead to flight performance that is worse than that predicted. In the case of the C-141, the wing pressure distribution in flight shows that the shock is further aft than predicted by the wind tunnel tests. This increased aft loading meant that the pitch characteristics of the wing were very different in flight to that predicted and this necessitated a complete re-design of the wing. There are many examples of where flight performance is worse than predicted using wind tunnel tests at lower Reynolds numbers, some of which are given by Wahls (2001). Examples include higher than expected interference drag of the F-111 airframe, the lack of performance benefit for the DC-10 using a drooped aileron and recently the wing-drop phenomenon of the F/A-18E/F Super Hornet (Stookesberry (2001)). The flight performance need not be worse than predicted from wind tunnel data, with the example given by Wahls (2001) of the increased cruise speed of the C-5A due to a delayed drag rise in flight.

The fact that the flight performance is better than predicted means that the design point was calculated incorrectly and raises the possibility that the design is overly conservative. The financial incentives for designing and predicting the flight performance of an aircraft at high Reynolds numbers are large. This is true not only for the aircraft manufacturer, who has to meet certain performance guarantees or face stiff financial penalties or a costly re-design, but also for the aircraft operator. Mack & McMasters (1992) reported that a 1% reduction in drag equates to several million dollars in savings per year for a typical fleet of aircraft. Bocci (1979) examined what performance might be lost by designing an aerofoil at a typical test Reynolds number of 6×10^6 instead of a typical full-scale Reynolds number of 35×10^6. The results were gained by calculating the 2D transonic flow over an aerofoil section, and it was found that:

(*a*) The C_L for the section designed (using CFD) to operate at $Re_c = 6 \times 10^6$, but simulated at $Re_c = 35 \times 10^6$ is 4% higher for the same Mach number and shock strength on the upper surface.

(*b*) For the aerofoil section designed (using CFD) for a Reynolds number of 35×10^6, the improvement in C_L is 13% over the section designed and simulated at a Reynolds number of 6×10^6.

The accurate prediction of flight performance would also save time in the development process by reducing the number of wind-tunnel hours, flight-test hours and design iterations. The use of CFD has helped reduce the upward trend in the number of wind-tunnel hours required to develop an aircraft (Beach & Bolino (1994)), although approximately 20,000 wind tunnel hours were still required to develop the Boeing 777-200.

Differences between predicted and flight performance have led to many different methods of simulating the flight Reynolds number flow using low Reynolds number testing facilities. In flight, transition normally occurs near the leading edge of the wing, and the boundary layer interacting with the shock wave is therefore turbulent. In wind tunnels, it is possible for the boundary layer to remain laminar over a large percentage of the chord, and therefore a laminar boundary layer-shock interaction may occur. These two types of interaction are vastly different in their nature, and therefore the flow is generally tripped. For many years the standard method of transition fixing was to place narrow, sparse bands of carborundum or ballotini at chordwise positions of between $0.05c$ and

0.07c. This worked well for many aerofoils pre-1960, but not for the highly-aft-loaded sections such as the C-141 where a trailing edge separation exists. The sensitivity of a type B flow to transition location and the degree of roughness is discussed by Haines (1987) for the NPL 9240 and 9241 sections, whose only difference is a very slight change in the upper-surface thickness aft of the point of maximum thickness. The pressure distribution of the NPL 9241 shows that a small incipient trailing-edge separation exists at Mach 0.6, which is not present for the NPL 9240. The $C_L - M$ plot for the two sections shows that when fine sparse roughness is used at 10-15% chord the behaviour of the two is similar. However, the differences are large when coarse roughness is used close to the leading edge, and the effects of a shock-induced separation on the break in the lift data are greater for the 9241 section.

The increased sensitivity of type B flows to scale effects led to steps being taken to simulate the high-Reynolds-number flow more accurately by reducing the non-dimensional boundary-layer thickness on the model to a value close to that found in flight. One method of achieving this is known as aft-fixing, allowing the boundary layer to remain laminar and thin over the forward part of the wing and then fixing transition aft of where it occurs naturally in flight, but far enough ahead of the shock wave to avoid any local interaction of the shock and the transition trip. This technique has proved to be capable of alleviating the rear separation found in model tests for $2 \times 10^6 < Re_c < 6 \times 10^6$, which are not expected to occur in flight (Haines (1987)).

Three-dimensional effects complicate the use of the aft-fixing technique on typical high-aspect-ratio transport aircraft wings. Near the wing root there is often a double-shock pattern with the intersection point to the single outboard shock often close to the kink-section of the wing. The leading shock in the double-shock pattern is often close to the leading edge of the wing, and therefore the aft-fixing technique will not be applicable. Furthermore, the transition mechanism in a three-dimensional flow is different from a two-dimensional flow where the Tollmien-Schlichting instability is the primary cause. In a three-dimensional flow, cross-flow instability and leading-edge contamination can also contribute to transition. Transition also occurs near to the leading edge at the wing tip, and therefore if the aft-fixing transition method is to be used on a swept wing, the trip strip must be cranked and then only the mid-section of the wing is represented adequately. Elsenaar (1988b) discusses the effect of transition fixing upon the local sweep angle of the shock, and how this is important for drag evaluation because of the sensitivity of compressibility drag to small variations in shock strength and sweep angle.

Alternative techniques to the aft-fixing method are discussed briefly by Elsenaar (1988b) and include vortex generators, boundary-layer suction and geometry modification on the sub-scale model. Haines & Elsenaar (1988) and Haines & Elsenaar (1988b) discuss detailed methodologies for simulating the full-scale behaviour of an aircraft wing using sub-flight Reynolds-number facilities, and moreover what the most important simulation criteria should be, given that it is unlikely to be able to simulate them all. The simulation criteria listed by Haines & Elsenaar (1988b) are:

(a) Shock position
(b) Shock strength
(c) Non-dimensional momentum thickness at the wing trailing edge
(d) Non-dimensional length of the shock-induced separation bubble
(e) Boundary-layer shape factor at a position close to the trailing edge on the upper surface, or at any other position where separations are anticipated

Even with complex simulation methodologies, the flight performance and character-

istics of an aircraft can be hard to predict using low-Reynolds-number facilities. This led to the recognition of the need for high-Reynolds-number testing facilities such as the National Transonic Facility (NTF) at NASA Langley and the European Transonic Windtunnel (ETW) in Cologne, Germany. Both tunnels can operate at cryogenic temperatures using Nitrogen and from low Mach numbers (0.15-0.2) to supersonic Mach numbers (1.2-1.3). Importantly, they can operate at Reynolds numbers greater than that achieved in flight by typical transport aircraft, and are capable of varying temperature, pressure and velocity independently, allowing the separation of Reynolds number effects from aeroelastic effects.

Despite the existence of the NTF and ETW, industrial and commercial wind tunnels are still required to carry out the majority of the development work for a new aircraft because of their relatively high productivity. The ETW and NTF are viewed as research tunnels where Reynolds-number scaling methodologies can be developed and an aircraft design checked before its first flight. The requirement for Reynolds-number scaling methods has therefore not diminished with the advent of high-Reynolds-number facilities.

To further understand the effects of scale upon aircraft performance and to establish a capability to account for them during the design process, the High Reynolds number Aerodynamic Research Project (HiReTT) was commenced in January 2000 as part of the European Fifth Framework Programme. This project combined with others funded by the EC is part of a strategy that aims to make European aeronautics the World leader by the year 2020 (Argüelles *et al.* (2001)).

The specific objectives of HiReTT are listed by Rolston (2001) and include the testing of a modern aircraft research configuration with and without control devices at high Reynolds numbers and particularly at high subsonic Mach numbers. The database gained will be fully corrected for interference effects by evaluating and developing new and existing methods in the ETW and by using CFD. The results from the ETW will also be compared with the predictions of modern CFD methods, with a view to producing guidelines to enable CFD to predict such flows.

The US does not at present have such a research program dedicated to Reynolds number scaling, although between 1994 and 2000 the NASA Advanced Subsonic Transport (AST) program funded research into Reynolds number scaling using the NTF. There is undoubtedly a great deal of experience in scaling techniques in the US, with 57% of research investigations in the NTF since 1985, concentrating on subsonic transport aircraft (Wahls (2001)). Much of the data and knowledge however remains undisclosed due to its proprietary nature.

The current status of Reynolds-number scaling can be assessed from a number of recent publications resulting from the use of the NTF (Curtin *et al.* (2002) and Clark and Pelkman (2001)) and ETW (Rolston (2001), Quest *et al.* (2002), and Hackett *et al.* (1999)). The full details are too long to discuss in this brief, but an attempt at a summary is provided herein.

(*a*) Angle of incidence at cruise, drag-rise Mach number, C_L and C_M are all functions of Reynolds number. Comparison of data from the NTF and ETW with flight measurements is very good for cruise conditions.

(*b*) The effect of Reynolds number on drag can be predicted if the empirical relationship is matched to drag measured at a Reynolds number of 8-10 million or above.

(*c*) The shape of drag polar varies with Reynolds number up to flight Reynolds numbers of approximately 40 million, although vortex generators reduce the variation slightly.

(*d*) Drag-rise Mach number is increased with increasing Reynolds number, indicating

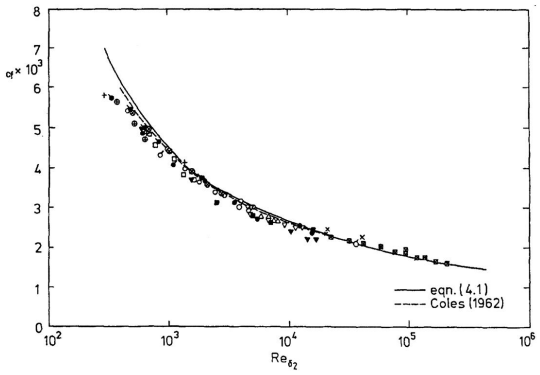

FIGURE 4. Comparison of flat plate skin friction data with the relationships of Fernholz (1971) and Coles (1962) (Fernholz & Finley (1996))

that higher Reynolds number testing would predict a higher cruise Mach number than that achieved using a tunnel such as the Boeing Transonic Wind Tunnel (BTWT).

(*e*) The effect of vortex generators on drag at cruise varies with Reynolds number, causing a higher drag at low Reynolds numbers and having very little or a slightly beneficial effect at flight Reynolds numbers. Vortex generators also have little effect on spanwise loading at flight Reynolds numbers, compared with a large effect at low Reynolds numbers. This indicates that if wing loads were developed from low Reynolds number data, an unnecessary structural weight penalty would be paid.

(*f*) Buffet onset is very difficult to predict, and is often difficult to measure in a wind tunnel because the model dynamics and that of the aircraft are very different.

Drag estimation is an important part of the design process, and involves the prediction of wave drag, vortex-induced drag and viscous drag, with the latter contributing approximately 50% to the total drag during cruise (Thibert *et al.* (1990)). A simple estimate of the scaled viscous drag is often gained by using a combination of form factors and flat plate skin friction formulae once the transition location is known. This method relies upon an accurate description of the skin friction coefficient, c_f from low Reynolds numbers found in wind tunnels to flight Reynolds numbers.

2. Skin friction estimation

There is a variety of empirical and semi-empirical relationships for the prediction of the turbulent incompressible skin friction on a flat plate. Common methods such as those based upon the $\frac{1}{7}$-th power law and the logarithmic law (Schlichting (1968)) relate c_f to Re_x and suffer from the difficulty of an unknown origin.

Fernholz & Finley (1996) compare measurements of flat-plate skin friction from a variety of sources for $300 < Re_\theta < 212 \times 10^3$ to the empirical relationship of Coles (1962) and the semi-empirical relationship of Fernholz (1971) as shown in figure 4. Agreement with the experimental data is within $\pm 5\%$ in the range $600 < Re_\theta < 212 \times 10^3$, although the agreement is better at higher Reynolds numbers.

More recently, Watson *et al.* (2000) carried out a comparison of the semi-empirical relationships of Ludwieg & Tillmann (1950), Spalding (1962), Kármán-Schoenherr (Schoenherr (1932)) and Fernholz (1971) as shown in figure 5. The methods of Kármán-Schoenherr and Spalding show opposite trends at low and high Reynolds numbers with the inter-

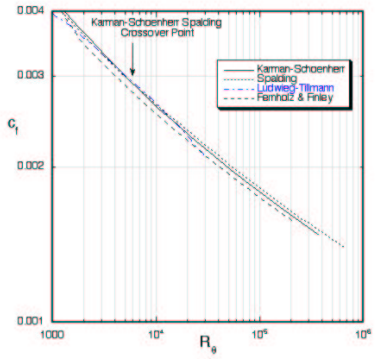

FIGURE 5. Flat plate skin friction correlations and theories (Watson *et al.* (2000))

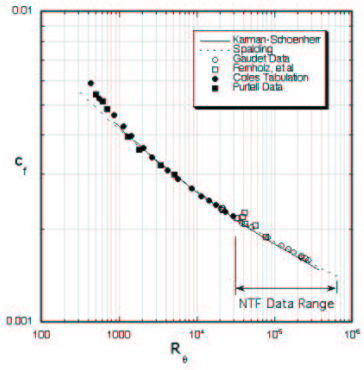

FIGURE 6. Comparison of the flat plate data with the correlations and theories (Watson *et al.* (2000))

section point at Re_θ between 6000 and 7000. The relationship of Fernholz consistently underpredicts the skin friction compared to the other methods. The skin friction predicted by Ludwieg-Tillmann matches that of Kármán-Schoenherr for Re_θ between 3000 and 20000. Both the methods of Spalding and Fernholz rely upon the logarithmic law and hence the von Kármán constant κ and the additive constant, B. Watson *et al.* (2000) report that the method of Spalding incorrectly predicts the skin friction if the usual value of κ is used. This is because the relationship relies upon Spalding's sublayer-buffer-log profile which does not take the wake region into account correctly. Despite this, the relationships of Kármán-Schoenherr and Spalding are observed to be the best fit to the data of Coles (1962) and Gaudet (1984) shown in figure 6.

The relationships of Spalding and Kármán-Schoenherr are used for comparison with the data taken in the National Transonic Facility (NTF) at NASA Langley in 1996. Although a flat-plate experiment was originally proposed by Saric & Peterson (1984), it posed too many problems in the high-dynamic-pressure environment of the NTF. An axisymmetric body, 17ft long, for which transverse-curvature effects are small ($\delta/R = 0.25$) was therefore tested at Mach numbers between 0.2 and 0.85 and unit Reynolds numbers from 6×10^6 to 94×10^6 per foot. Skin friction was measured using three different techniques: a skin friction balance, Preston tubes and velocity profiles from which the skin friction was inferred by the Clauser method. The last method relies upon the validity of the logarithmic law and the constants used, which have been a subject of debate over the last decade, and one that is still not settled. Hites *et al.* (1997) compared the skin friction velocity u_τ measured by a near-wall hot wire, a microfabricated hot wire on the wall, and a conventional hot wire on the wall to that obtained by measuring the velocity profile using a hot wire and applying the Clauser technique. In all cases, the measured u_τ is higher than that predicted by the Clauser technique. The prediction of u_τ is also sensitive to the values of κ and B used in the log-law, with a ± 0.5 change in the slope $1/\kappa$ resulting in a 12% difference in u_τ. The comparison of the measured values of u_τ to that predicted by the Clauser method should however be treated with care as significant errors can occur, even for microfabricated devices, due to thermal conduction to the substrate and connecting wires.

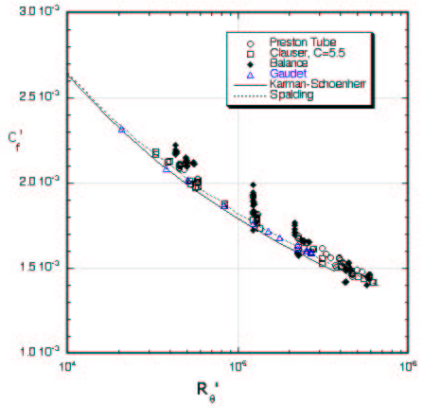

FIGURE 7. Comparison of three measurement techniques of skin friction with the data of Gaudet (1984) and with the predictions of Kármán-Schoenherr and Spalding (Watson *et al.* (2000))

Compressibility effects on the skin friction are removed using the van Driest transformation (Van Driest (1951)) for the velocity-profile data and the Sommer and Short T' method (Sommer & Short (1955)) for the Preston-tube data. Using the Van Driest transformation for the velocity profile at the highest Reynolds number condition yielded an incompressible Re_θ of 619,800.

Data obtained using the skin friction balance exhibits a large degree of scatter and these data were therefore not relied upon. The data from the Preston tubes and velocity profiles shows good agreement, and yields a best fit relationship of $c_f = 0.0097 Re_\theta^{-0.144}$ shown in figure 7. The scatter of the data around this fit is $\pm 1\%$, with the fit 1% above the Spalding value and 3% above the Kármán-Schoenherr value at Re_θ=600,000. It equals the Spalding value at Re_θ=30,000.

Skin friction measured in two facilities using the near-wall technique and oil-film interferometry is compared by (Österlund *et al.* (1999)) for Re_θ up to 27000. The data compare well with the correlation of Fernholz (1971) and the logarithmic skin-friction law using $\kappa = 0.384$ and $B = 4.08$. However, the range of Re_θ considered is too small, and the maximum Reynolds number too low, to draw conclusions about the suitability of the correlation and logarithmic skin friction law at high Reynolds number.

3. Conclusions

Reynolds number scaling remains a topic that receives a great deal of attention 50 years after such effects were first observed. The advent of high Reynolds number tunnels such as the NTF and ETW has not lessened the need for good Reynolds number scaling techniques, but has provided the facilities in which to test new methods and aircraft designs before their first flight, helping to reduce risk. Comparison of flight data with that taken in such tunnels is good for cruise conditions. However, buffet onset is still very difficult to predict, due primarily to the fact that the wind tunnel model and support dynamics are very different to the real aircraft.

The accurate prediction of drag at flight Reynolds number using low Reynolds number wind tunnels remains a challenge, and it appears that a Reynolds number of 8-10 million or above is required if empirical methods are to be used for extrapolation to flight conditions. The error in the extrapolation is likely to be higher than the variation of c_f with Reynolds number predicted by the best empirical methods discussed. It is therefore concluded that the measurements of skin friction taken in the NTF over a very large range of Reynolds number match the predictions of Spalding and Kármán-Schoenherr well enough for skin friction extrapolation purposes. The direct and accurate measurement of skin friction however remains very challenging, although microfabricated skin friction devices are proving promising.

REFERENCES

Argüelles, P., Bischoff, M., Busquin, P., Droste, B. A. C., Evans, R., Kröll, W., Lagardére, J-L., Lina, A., Lumsden, J., Ranque, D., Rasmussen, S., Reutlinger, P., Robins, R., Terho, H. & Wittlöv, A. 2001 European aeronautics: A vision for 2020. European Commission.

Beach, H. L., Jr. & Bolino, J. V. 1994 National planning for aeronautical test facilities. *AIAA Paper* 94-2474.

Bocci, A. J. 1979 Aerofoil design for full scale Reynolds number. *ARA Memo* 211.

Clark, R. W. & Pelkman, R. A. 2001 High Reynolds number testing of advanced transport aircraft wings in the National Transonic Facility. *AIAA Paper* 2001-0910.

Coles, D. 1962 The turbulent boundary layer in a compressible fluid. *R-403-PR*, Rand Corp.

Curtin, M. M., Bogue, D. R., Om, D., Rivers, S. M. B., Pendergraft, O. C., Jr., & Wahls, R. A. 2002 Investigation of transonic Reynolds number scaling on a twin-engine transport. *AIAA Paper* 2002-0420.

Elsenaar, A. Observed Reynolds number effects: Airfoils and high aspect ratio wings. Elsenaar, A., Binion, T. W. & Stanewsky, E. 1988 Reynolds number effects in transonic flow. *AGARDograph AG-303*, 17-49.

Elsenaar, A. Introduction. Elsenaar, A., Binion, T. W. & Stanewsky, E. 1988 Reynolds number effects in transonic flow. *AGARDograph AG-303*, 1-6.

Fernholz, H. H. 1971 Ein halbempirisches Gesetz für die Wandreibung in kompressiblen turbulenten Grenzschichten bei isothermer and adiabater Wand. *ZAMM.* **51**, 149-149.

Fernholz, H. H. & Finley, P. J. 1996 The incompressible zero-pressure gradient turbulent boundary layer: An assessment of the data. *Prog. Aerospace Sci.* **32**, 4, 245-311.

Gaudet, L. 1984 Experimental investigation of the turbulent boundary layer at high Reynolds number and a Mach number of 0.8. *TR 84094*, Royal Aircraft Establishment.

Hackett, K., Burnell, S. & Ashill, P. 1999 Aerodynamic scale effects on a transport aircraft model at high subsonic speed. *AIAA Paper* 99-0305.

Haines, A. B. 1987 27th Lanchester memorial lecture: Scale effect in transonic flow. *Aeronautical Jnl.*, August/September 1987, 291-313.

Haines, A. B. 1994 Scale effects on aircraft and weapon aerodyamics. *AGARDograph AG-323.*

Haines, A. B. & Elsenaar, A. 1988 An outline of the methodology. Boundary layer simulation and control in wind tunnels. *AGARD Advisory Report AR-224*, 96-110.

Haines, A. B. & Elsenaar, A. 1988 Transport-type configurations. Boundary layer simulation and control in wind tunnels. *AGARD Advisory Report AR-224*, 139-163.

Hall, M. G. 1971 Scale effects in flows over swept wings. *AGARD CP 83-71.*

Hites, M., Nagib, H. & Wark, C. 1997 Velocity and wall shear stress measurements in high Reynolds number turbulent boundary layers. *AIAA Paper* 97-1873

Ludwieg, H. & Tilmann, W. 1950 Investigations of the wall shearing stress in turbulent boundary layers. *NACA TM-1285.* National Advisory Committee for Aeronautics.

Mack, M. D. & McMasters, J. H. 1992 High Reynolds number testing in support of transport airplane development. *AIAA Paper* 92-3982.

Österlund, J. M., Johansson, A. V., Nagib, H. M. & Hites, M. H. 1999 Wall shear stress measurements in high Reynolds number boundary layers from two facilities. *AIAA Paper* 99-3814.

Pearcey, H. H. & Holder, D. W. 1954 Examples of shock induced boundary layer separation in transonic flight. *Aeronautical Research Council Technical Report R & M No. 3012.*

Pearcey, H. H., Osborne, J. & Haines, A. B. 1968 The interaction between local effects at the shock and rear separation - a source of significant scale effects in wind tunnel tests on aerofoils and wings. *AGARD CP 35*, Paper 11.

Quest, J., Wright, C. N. & Rolston, S. 2002 Investigation of a modern transonic transport aircraft configuration over a large range of Reynolds numbers. *AIAA Paper* 2002-0422.

Rolston, S. 2001 High Reynolds number tools and techniques for civil aircraft design. *AIAA Paper* 2001-2411.

Saric, W. S. & Peterson, J. B., Jr. 1984 Design of high Reynolds number flat plate experiments in the NTF. *AIAA Paper* 84-0588.

Schlichting, H. 1968 *Boundary Layer Theory.* McGraw-Hill.

Schoenherr, K. E. 1932 Resistance of flat surfaces moving through a fluid. *Trans. SNAME.* **40**, 279-313.

Sommer, S. C. & Short, B. J. 1955 Free-flight measurements of turbulent boundary layer skin friction in the presence of severe aerodynamic heating at mach numbers from 2.8 to 7.0. *NACA TN-3391.*

Spalding, D. B. 1962 A new analytical expression for the drag of a flat plate valid for both turbulent and laminar regimes. *Int. Jnl. Heat and Mass Transf.* **5**, 1133-1138.

Stookesberry, D. 2001 CFD modeling of the F/A-18E/F abrupt wing stall - a discussion of the lessons learned. *AIAA Paper* 2001-2662.

Thibert, J. J., Reneaux, J. & Schmitt, R. V. 1990 ONERA activities on drag reduction. *Proceedings of the 17th Congress of the ICAS.* 1053-1059.

van Driest, E. R. 1951 Turbulent boundary layer in compressuble fluids. *Jnl. Aeronautical Sci.* **18**, 3, 145-160.

Wahls, R. A. 2001 The National Transonic Facility: A research retrospective. *AIAA Paper* 2001-0754.

Watson, R. D., Hall, R. M. & Anders, J. B. 2000 Review of skin friction measurements including recent high Reynolds number results from NASA Langley NTF. *AIAA Paper* 2000-2392.